JOURNAL OF CATALYSIS 111, 286–295 (1988)

Comparison of the Acidities of WO_3/Al_2O_3 and Ultrastable Faujasite Catalysts

S. L. SOLED,*,† G. B. MCVICKER,*,‡ L. L. MURRELL,*,§ L. G. SHERMAN,*,‖ N. C. DISPENZIERE, JR.,* S. L. HSU,¶ AND D. WALDMAN¶

*Exxon Research and Engineering Company, Route 22 East, Annandale, New Jersey 08801; and ¶University of Massachusetts, Amherst, Massachusetts 01003

Received July 17, 1987; revised January 4, 1988

The acidity of WO_3 on γ-alumina is compared with that of ultrastable faujasite using both base adsorption techniques and model compound conversion studies. The addition of WO_3 to γ-alumina introduces Brønsted acidity, and the density of Brønsted sites is increased by high-temperature calcination. The acid sites displayed by the supported tungsten oxide catalyst are considerably weaker than those found in ultrastable faujasite. © 1988 Academic Press, Inc.

INTRODUCTION

Supports often modify the properties of supported transition metal oxides. For example, silica stabilizes Cr(VI) at temperatures above which bulk chromic anhydride decomposes (*1*). Recently several research groups have reported that tungsten oxide strongly interacts with γ-Al_2O_3 (*2–5*), influencing the properties of both the WO_3 and the γ-Al_2O_3 components. We have previously reported on temperature-programmed reduction, controlled atmosphere electron microscopy, ESCA, and laser Raman spectroscopy studies of WO_3 on Al_2O_3 (*6*). These earlier studies suggested that below monolayer coverage a difficult to reduce, highly dispersed surface tungsten oxide complex exists, whereas at higher coverages an additional easily reduced bulk-like WO_3 species is also present.

Bulk tungsten oxide exhibits acidic functionality in *n*-heptane hydrocracking (*7*), olefin isomerization (*8*), and alcohol dehydration (*9*) reactions. Mixed metal oxides such as Al_2O_3–TiO_2 (*10*), as well as supported metal oxides such as MoO_3 on Al_2O_3 or WO_3 on Al_2O_3 (*11–13*), also display acidic properties. We have investigated the acidity of the WO_3 on Al_2O_3 system and compared it with that of ultrastable faujasite (hereafter designated as ultrastable FAU). We used high-temperature gravimetric titration of amines, temperature-programmed desorption of NH_3, and infrared spectroscopy of adsorbed pyridine to monitor the number, type, and relative strengths of the acid sites.

Additionally, model compound conversion studies employing isobutane and 2-methyl-2-pentene served as acidity probes and provided a basis of comparison with gas oil cracking. The acidity of the tungsten oxide surface complex is contrasted with that of a microporous zeolitic acid and a model is proposed to account for the observed differences. Finally, we describe the tungsten oxide surface coverage which yields optimum stability and acidity.

EXPERIMENTAL

Surface areas were determined by a multipoint BET measurement using N_2 adsorption. The framework Si/Al ratio in ultrastable FAU was determined by ^{29}Si MAS NMR measurements (*14*). Base titrations

† Present address: Sunstone, Plainsboro, NJ 08536.
‡ To whom all correspondence should be addressed.
§ Present address: Engelhard, Specialty Chemicals Division, Menlo Park, NJ 08818.
‖ Present address: 3 Honeyman Drive, Flemington, NJ 08822.

0021-9517/88 $3.00

with 3,5- and 2,6-lutidine (dimethylpyridines) were measured on a Mettler TA 2000C. Prior to base adsorption, samples were calcined in helium at 500°C until constant weight was achieved. The temperature was lowered to 250°C, and an aliquot of lutidine in excess of the equilibrium amount was injected via a microsyringe through a heated port directly into the sample area. Physically adsorbed lutidine was differentiated from chemically adsorbed lutidine as described previously (*15*). Adsorptions were sequentially measured at 250, 200, and 150°C. No discoloration of the catalyst due to decomposition of the basic adsorbate was observed.

Desorption measurements of NH_3 were performed by coupling a Leybold Heraeus Binos infrared gas analyzer to the thermal balance. The Binos analyzer measures a differential flow between the reference and the sample chamber. Sensitivity ranged from 0 to 5000 ppm. The sample was calcined at 600°C under He and allowed to cool to room temperature; NH_3 was then introduced and the subsequent desorption under He was programmed at 12°C/min to 600°C.

Infrared absorption spectra were collected on an IBM 98 Fourier transform spectrometer with an MCT detector. A controlled atmosphere high-temperature diffuse reflectance accessory (Harrick Scientific) was placed in the spectrometer sample chamber. Powdered samples (~100 mg) were calcined in N_2 at 500°C for 2 h, cooled to 150°C, and exposed for 30 min to N_2 (150 cm^3/min) saturated with dry pyridine at room temperature. The cell was then evacuated at this temperature for 4 h to remove physically adsorbed pyridine. One thousand infrared scans were collected. Following data collection, the sample temperature was raised to 250°C, desorbed pyridine was removed under vacuum (1 h), and a second infrared spectrum was recorded. A similar treatment at 400°C followed.

WO_3 on γ-Al_2O_3 catalysts were prepared by the incipient wetness impregnation of γ-Al_2O_3 with ammonium *meta*-tungstate solutions. The reforming grade γ-alumina, obtained from Engelhard Industries, was precalcined at 500°C and exhibited a surface area of 184 m^2/g.

The supported WO_3 catalysts were calcined at either 500 or 950°C for 18 h. The ultrastable FAU catalyst (LZ-Y82) was obtained from Linde.

Isobutane and 2-methyl-2-pentene conversions were carried out in a fixed-bed microreactor operated under differential conditions. Experimental conditions are outlined in separate publications (*16, 17*). Gas oil cracking activities were measured on a standard MAT unit equipped with steam injection (*18*).

RESULTS AND DISCUSSION

1. Catalysts

Table 1 lists surface areas for the catalysts employed in these studies. For ultrastable FAU, the bulk Si/Al ratio was determined by analyses to be 2.7; ^{29}Si MAS NMR sets the framework Si/Al ratio to be near 5.0. This difference indicates that substantial nonframework alumina is present in the zeolite. The cell constant of the ultrastable FAU is 24.56 Å and the residual sodium content, as Na_2O, is 0.2 wt%.

2. TG Amine Titrations

Thermogravimetric titrations with two amines of approximately equal base strength but different steric hindrances (2,6- and 3,5-dimethylpyridine) provide a semiquantitative comparison of Lewis and Brønsted acid site density. As first sug-

TABLE 1

Surface Areas of Solid Acid Catalysts

Catalyst	Calcination temperature (°C)	Surface area (m^2/g)
γ-Al_2O_3	500	184
10% WO_3/γ-Al_2O_3	500	184
10% WO_3/γ-Al_2O_3	950	80
Ultrastable FAU	500	770

TABLE 2

Lutidine Titration Results

Catalyst	Calcination temperature (°C)	3,5-Dimethylpyridine						2,6-Dimethylpyridine					
		μmol/g			μmol/m²			μmol/g			μmol/m²		
		150°C	200°C	250°C	150°C	200°C	250°C	150°C	200°C	250°C	150°C	200°C	250°C
γ-Al_2O_3	500	375	277	207	2.03	1.51	1.13	166	102	60	0.90	0.55	0.33
10% WO_3/γ-Al_2O_3	500	367	276	214	1.99	1.50	1.16	185	127	90	1.01	0.69	0.49
10% WO_3/γ-Al_2O_3	950	155	121	93	1.94	1.51	1.16	98	74	56	1.23	0.93	0.70
Ultrastable FAU	500	2006	1759	1496	2.61	2.28	1.94	1625	1397	1059	2.11	1.81	1.38

gested by Brown and Johanneson (*19*) and later applied by Benesi and Winquist (*20*), 2,6-dimethylpyridine acts as a selective probe for Brønsted sites, whereas the less hindered 3,5-dimethylpyridine reacts with both types of acid sites. Table 2 presents the titration data for the γ-Al_2O_3, WO_3 on γ-Al_2O_3, and ultrastable FAU catalysts. Note that some 2,6-lutidine does adsorb on γ-Al_2O_3 even though only Lewis sites are thought to exist on this material (*21, 22*). Hence, this titrant is not a totally selective probe of Brønsted acidity. Consequently, comparative titrations with the hindered amine can be interpreted only semiquantitatively. The total acid site densities of the alumina and tungsten oxide on alumina catalysts remain approximately the same, whereas the fraction of Brønsted character increases with both tungsten addition and high-temperature calcination. The ultrastable FAU catalyst contains a 1.3- to 1.7-fold higher total acid site density and a 2 to 3 times higher Brønsted site density than the tungsten catalysts. The majority of acid sites in the ultrastable FAU are Brønsted in nature. The Lewis sites displayed by the zeolite may be associated with the detrital alumina phase.

3. *Temperature-Programmed Desorption of NH_3*

Temperature-programmed desorption (TPD) of NH_3 was employed as a qualitative probe of the overall acid site strength. Since the TPD of a base represents a dynamic measurement of a thermodynamic property, care must be exercised in interpreting results (*23, 24*); we choose to view the TPD results only qualitatively. NH_3 functions as a non-site-specific base; hence, it reflects the total acid site strength in a particular sample.

Figure 1 shows the NH_3 desorption results from the γ-Al_2O_3, WO_3 on γ-Al_2O_3, and ultrastable FAU (zeolite Y) solid acids. Only minor differences among the tungsten oxide and alumina catalysts appear. NH_3 desorbs in one large envelope centered near 150°C. γ-Al_2O_3 holds onto the adsorbed NH_3 more strongly than the tungsten catalysts, suggesting the presence of slightly stronger acid sites. For the ultrastable FAU, however, notable differences occur. In addition to the large envelope of physically and weakly chemisorbed ammonia at low temperature (~135°C), two high-temperature desorption peaks occur, including one near 450°C. The high-temperature peaks suggest that stronger sites exist on the Y zeolite than on the WO_3 on γ-Al_2O_3 catalysts. Comparative thermal desorption experiments with a hindered pyridine base would prove instructive; however, the alkyl groups are cracked from the pyridine ring at elevated desorption temperatures. As is discussed later this acid strength difference between supported WO_3 and ultrastable FAU catalysts produces dramatic contrasts in their reaction chemistry.

4. *Infrared Studies of Adsorbed Pyridine*

Since the TPD data suggested that acid site strength differences among γ-Al_2O_3,

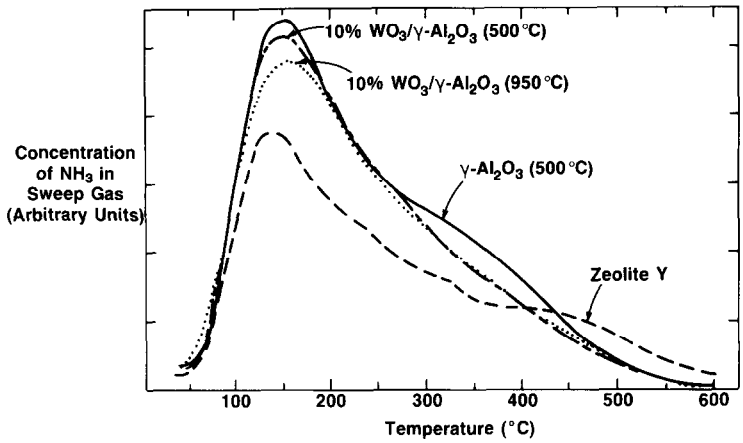

FIG. 1. Temperature-programmed desorption of NH_3.

WO_3 on γ-Al_2O_3, and ultrastable FAU exist, we examined the infrared spectrum of pyridine adsorbed on these materials. In the wavelength region between 1400 and 1700 cm^{-1} the spectrum of adsorbed pyridine provides characteristic bands for both coordinatively bound Lewis-type pyridine molecules and protonated Brønsted-type pyridinium ions (*25–27*). Monitoring changes in peak intensity with temperature allows a qualitative comparison of the relative site acid strengths. Comparison of the pyridine infrared spectra measured at 150°C of γ-Al_2O_3 (500°C calcined), 10% WO_3 on γ-Al_2O_3 (500°C calcined), and 10% WO_3 on γ-Al_2O_3 (950°C calcined) catalysts in the 1400–1700 cm^{-1} region are given in Fig. 2. For γ-Al_2O_3 the strong bands near 1450 and 1580 cm^{-1} result from Lewis-bound pyridine. Bands near 1540 and 1635 cm^{-1}, which would indicate Brønsted pyridinium ions, are not present. Their absence is consistent with previous reports (*25–27*). Consequently overlapping bands at 1490 and 1620 cm^{-1} are assigned to Lewis sites. For the WO_3 on γ-Al_2O_3 catalyst calcined at 500°C, Brønsted bands at 1540 and 1635 cm^{-1} begin to appear. Following calcination at 950°C the Brønsted bands increase in intensity. Although the extinction coefficients for the Lewis versus Brønsted sites for these materials are not known, it is reasonable to conclude that Brønsted acidity appears on the 500°C calcined WO_3 on γ-Al_2O_3 catalyst and increases upon high-temperature (950°C) calcination. This result agrees well with the previously described titration measurements. WO_3 on Al_2O_3 solid acids differ dramatically from other solid acids such as zeolites or amorphous silica–aluminas in that the Brønsted acidity increases at the expense of Lewis acidity upon high-temperature treatment. More

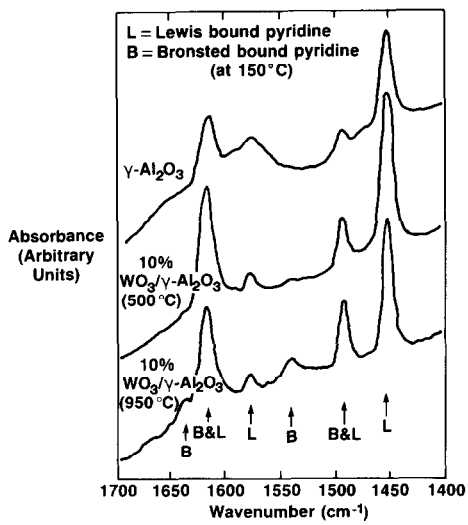

FIG. 2. "Drift" spectra of pyridine adsorption (150°C): alumina-based catalysts.

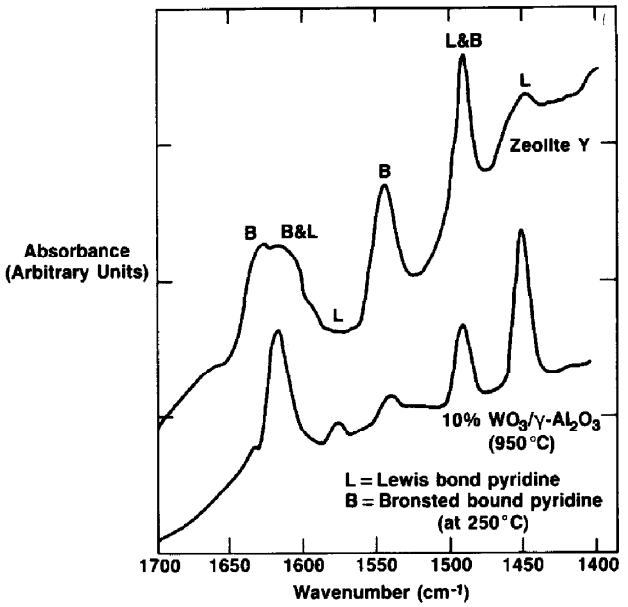

FIG. 3. "Drift" spectra of pyridine adsorption (250°C): ultrastable FAU vs WO_3/Al_2O_3.

conventional solid acids generate Lewis sites via dehydration of Brønsted sites during high-temperature calcinations.

Figure 3 contrasts the infrared spectra (measured at 250°C) of the ultrastable FAU (zeolite Y) with that of WO_3 on γ-Al_2O_3 calcined at 950°C. Note that for the Y zeolite Brønsted-type absorptions dominate, with only small bands being assignable to Lewis sites. Qualitatively, the infrared results agrees well with the TG titrations.

Comparison of the decrease in intensity of the Lewis and Brønsted sites with increasing desorption temperature is given in Fig. 4. For the WO_3 on γ-Al_2O_3 catalyst (950°C calcined) the Lewis sites are more strongly retained than the Brønsted sites. By 400°C, about 40% of the intensity at the Brønsted peak remains whereas 60% of the intensity of the Lewis peak remains. The Lewis sites on γ-Al_2O_3 also appear somewhat stronger than either of the sites on the

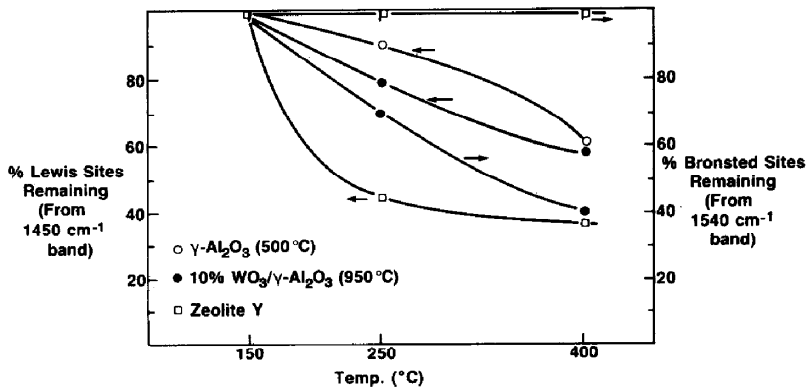

FIG. 4. Percentage of Lewis and Brønsted sites remaining at 250 and 400°C.

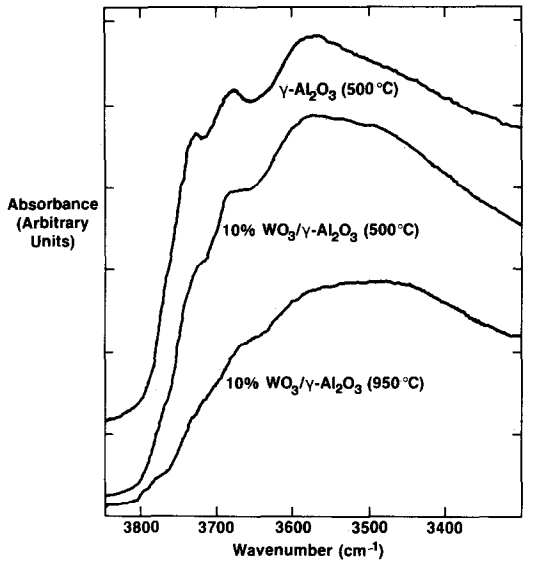

FIG. 5. "Drift" spectra of "OH" region (150°C).

tungsten-containing catalysts. TPD spectra suggested a similar ranking. Thus, differences in the type of acid site rather than large differences in their strength seem to distinguish the tungsten-containing catalysts from γ-Al_3O_3.

Whereas the number of Lewis sites on the ultrastable FAU (zeolite Y) sample capable of retaining pyridine decreases substantially with temperature, the intensity of the Brønsted peaks does not change. Contrast this behavior with the substantial decrease in Brønsted acidity for WO_3 on γ-Al_2O_3. Thus we conclude that Brønsted sites on ultrastable FAU are stronger than those on WO_3 on γ-Al_2O_3. This conclusion is consistent with the previously discussed TPD results.

The OH stretching region for the solid acids is presented in Fig. 5. The spectrum of γ-Al_2O_3 exhibits at least three different bands. Previously reported spectra identify three to five different types of OH stretching frequencies depending on sample and experimental conditions (*28, 29*). Knozinger has rationalized these findings by noting that in the (111) and (100) planes of γ-Al_2O_3 five distinct types of OH environments are present: OH coordinating to a single tetrahedral Al^{3+} ion, OH coordinating to a single octahedral ion, OH linking either a tetrahedral and octahedral aluminum ion or two octahedral ions, or finally, OH bridging three octahedral aluminum ions (*21*). These structurally different OH groups possess different binding energies and stretching frequencies. As WO_3 is loaded onto the γ-Al_2O_3 surface, the OH intensities decrease with increasing calcination temperature. In the case of the 950°C calcined sample, resolved OH stretches virtually disappear. Unfortunately, these measurements do not clearly indicate where the Brønsted sites on WO_3 on γ-Al_2O_3 catalysts are located. This remains an open question.

5. Reaction Studies with Isobutane and 2-Methyl-2-pentene

The selectivity of isobutane to cracked, isomerized, or alkylated products should reflect the observed differences in acid strengths between WO_3 on γ-Al_2O_3 and ultrastable FAU catalysts. On the other hand, the conversion of 2-methyl-2-pentene should provide a sensitive probe for changes in Brønsted acid site number or strengths within the series of supported tungsten oxides. Table 3 summarizes the major differences in the conversion of isobutane over the four solid acids. McVicker *et al.* have published a detailed study on this probe reaction (*16*). While conversion differences could be rationalized in part by enhanced adsorption of isobutane on the ultrastable FAU, as well as by acidity differences, the selectivity differences are dramatic. Secondary reaction products characteristic of carbonium ion chemistry (i.e., isomerization to *n*-butane, alkylation, and back cracking to $C_3^0 + C_5^0$) clearly distinguish the ultrastable FAU from the other solid acids. In the latter materials, only initial, radical-like products predominate. Since only minor acid site strength differences exist between the 500 and 950°C calcined WO_3 on Al_2O_3 samples, large selectivity differences in the isobutane con-

TABLE 3

Conversion of Isobutane

		γ-Al_2O_3	10% WO_3/γ-Al_2O_3 (500°C calcined)	10% WO_3/γ-Al_2O_3 (950°C calcined)	Ultrastable FAU
Conversion rate (at 550°C, relative to quartz beads)		84	200	54	3300
T(°C)		550	550	550	500
Conversion (%)		3.1	6.1	1.7	26.9
Selectivities (%)					
Secondary products	*n*-Butane	—	—	1.1	30.7
	Propane	Tr	0.5	0.6	34.0
	C_5^+	Tr	1.5	—	20.7
Initial products	Methane	9.6	6.9	3.5	2.4
	Propenes	24.4	24.4	13.5	2.8
	Butenes	65.6	65.6	79.4	5.8
	Other	0.4	1.1	1.9	3.6
H/C ratio		2.19	2.14	2.08	2.52

version patterns were not expected for the two WO_3 on Al_2O_3 materials.

Table 4 summarizes the 2-methyl-2-pentene isomerization data. The rate of the kinetically difficult methyl group migration (3M2P) is compared to the rate of the more facile double bond migration (4M2P) (*17*). For this reaction the increasing degree of Brønsted acidity in the WO_3 on γ-Al_2O_3 vs γ-Al_2O_3 catalysts parallels the increasing value of this isomerization ratio. High-temperature calcination of WO_3 on Al_2O_3 also increases this ratio. Note that the ultrastable FAU is such a strong acid that it quickly cokes and deactivates in this reaction test. Consequently, this test is not generally applicable to zeolites.

Isobutane conversion patterns appear to depend on Brønsted acid strength and clearly indicate that the stronger Brønsted sites in ultrastable FAU enable carbonium ion reactions to occur. The weaker Brønsted sites on WO_3 on γ-Al_2O_3 do not promote the typical carbonium ion reactions expected from this probe molecule. Isomerization of 2-methyl-2-pentene (i.e., methyl

TABLE 4

Isomerization of 2-Methyl-2-pentene over WO_3 on Al_2O_3

Catalyst	Conversion (mol%)	Apparent rates[a] (mol/h/g × 10^3)			Rate ratio[b] 3M2P/4M2P	MAT activity[c]
		2M1P	4M2P	3M2P		
γ-Al_2O_3	28.5	7.75	0.17	0.006	0.035	10
10% WO_3/γ-Al_2O_3 (500)	48.1	4.50	3.52	3.12	0.89	24
10% WO_3/γ-Al_2O_3 (950)	51.3	3.80	3.25	4.30	1.32	44

Note. Conditions: 101 kPa total pressure, 7.1 kPa 2M2P in He (150 cm^3/min), 250°C, 1.0 g catalyst, 1 h on feed.

[a] 2M1P, 2-methyl-1-pentene; 4M2P, *cis*- and *trans*-4-methyl-2-pentene; 3M2P, *trans*-3-methyl-2-pentene.

[b] Ratio increases with increasing Brønsted acid strength.

[c] Standard ASTM test D3907-80.

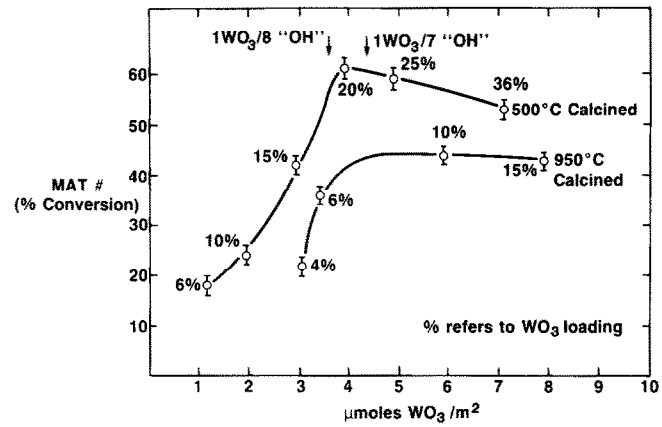

FIG. 6. MAT activity as a function of WO_3 loading.

group shift), in contrast, appears to parallel the increasing amount of Brønsted character in the WO_3 on γ-Al_2O_3 catalysts which occurs with increasing calcination severity. In this respect the hexene isomerization probe reaction results closely resemble those of gas oil cracking over WO_3 on Al_2O_3 catalysts.

6. *Gas Oil Cracking*

Gas oil cracking experiments were used to determine the effects of different WO_3 loading levels and catalyst calcination temperatures. After both 500 and 950°C calcinations the MAT activity increases and then plateaus or declines slightly as the WO_3 loading increases (Fig. 6). Activities pass through a maxima near 20% loading for the 500°C sample and near 7% for the 950°C calcined sample. From a recently proposed model, the density of "OH" sites on a completely hydroxylated (111) plane of γ-Al_2O_3 is estimated to be 30 μmol/m^2 (*31*). Thus, as the WO_3 density approaches one WO_3 group per seven OH sites the activity reaches a maximum. Interestingly, this also appears to be the optimum loading for inhibiting both the transformation of the transitional aluminas to α-alumina in inert or oxidizing environments and the reduction of WO_3 in reducing environments (*31*, *32*).

Tittarelli *et al.* report that during high-temperature calcination (1050°C) of WO_3 on γ-Al_2O_3, α-Al_2O_3 forms with WO_3 loadings less than 7–8%, and $Al_2(WO_4)_3$ forms for WO_3 loadings greater than 7–8%, whereas at 7–8% WO_3 loadings, a stable surface phase suppresses conversion of the transitional alumina to α-Al_2O_3 (*3*). Soled *et al.* have shown that during a 2-h 900°C H_2 reduction only small amounts of WO_3 reduce on 6% WO_3 on Al_2O_3 whereas close to 50% reduction to tungsten metal occurs for a 10% WO_3 on Al_2O_3 (*32*).

Thus, the reaction chemistry, transitional alumina stability, and tungsten oxide reduction resistance all indicate that optimum surface stability and acidity result when one WO_3 group occupies approximately one in every seven available surface OH sites.

PROPOSED ACID SITE MODEL

Figure 7 represents an idealized (111) plane of the alumina surface with the cubic close-packed anion layer exposed. We postulate that the WO_3 group will coordinate with either one or two surface OH groups. In either case we can envision the seven surface sites associated with a WO_3 center forming either a new Lewis or Brønsted site associated with the WO_3. The Lewis site would assume the configuration shown in Scheme 1a with the coordinatively unsatu-

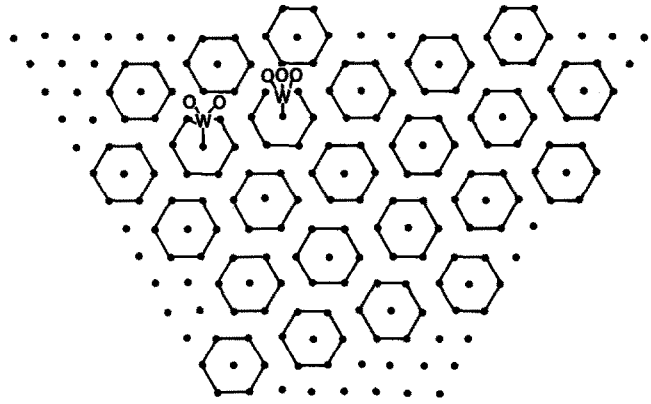

FIG. 7. Hypothetical packing arrangement of (111) face of WO_3/γ-Al_2O_3.

rated W center able to complex a Lewis base. The Brønsted site could assume the configuration shown below (b) with a proton available to react with a base. Our data suggest that the collapse of the alumina surface area and the increase in WO_3 site density with increasing calcination severity favor configuration (b) over (a) in Scheme 1.

Figure 7 shows how adjoining hexagonal areas enclosing anion sites in turn can close pack with neighboring hexagons. Our data suggest that this surface WO_3 geometry produces optimum stability and acidity with WO_3 on γ-Al_2O_3 catalysts.

The stronger Brønsted acidity of ultrastable FAU can be rationalized by a simple delocalization argument. If the Brønsted sites in the WO_3 on γ-Al_2O_3 assume configuration (b) in Scheme 1, the proton can delocalize only over three oxygen anions. In the zeolite structure the proton can delocalize over a larger number of anions. Increasing delocalization of the proton will stabilize the conjugate base and hence make the conjugate acid stronger.

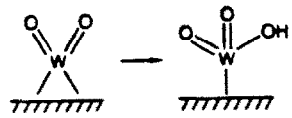

a b

SCHEME 1

A recent paper reports first principle local density pseudopotential calculations for describing acid sites on supported oxides by a cluster model (*32*). The calculations relate Brønsted acidity to the number of terminal oxygens and charge delocalization. The calculations are consistent with the results presented here.

CONCLUSIONS

We have found that the addition of WO_3 to γ-Al_2O_3 increases the Brønsted site density (per m^2) at the expense of Lewis sites while maintaining the density of total sites constant. Increasing the fraction of Brønsted sites by high-temperature calcination provides the WO_3 on Al_2O_3 catalysts their unique catalytic properties. WO_3 titrates the strongest Lewis sites on γ-Al_2O_3 and forms new Lewis or Brønsted sites that are slightly weaker. At the point where the Al_2O_3 surface is close-packed with WO_3 groups, the surface Al–OH groups are almost completely removed.

Ultrastable FAU contains about 1.5 times the total acid site density as the WO_3 on γ-Al_2O_3 but 2 to 3 times the Brønsted site density. The Brønsted sites on the Y zeolite are much stronger than any of the sites on the γ-Al_2O_3 or WO_3 on γ-Al_2O_3 catalysts. Because of this strength, secondary, carbo-

nium ion products predominate during isobutane conversion over ultrastable FAU, whereas, primarily initial, radical-like products are obtained over WO_3 on γ-Al_2O_3 catalysts.

The increasing Brønsted site density that occurs with WO_3 addition and high-temperature calcination parallels the increasing ability of the catalysts to shift methyl groups relative to double bonds in 2-methyl-2-pentene isomerization tests. This test may also reflect subtle strength increases with the high-temperature calcined WO_3 on γ-Al_2O_3 catalyt. The MAT gas oil cracking test parallels the 2-methyl-2-pentene isomerization test. A WO_3 loading of about one WO_3 group per seven surface anion sites results in the most stable and acidic surface, with WO_3 surface groups that are resistant to high-temperature reduction in hydrogen.

ACKNOWLEDGMENTS

The authors thank J. J. Ziemiak, H. Vroman, R. Jarmin, and B. DeRites for their assistance and G. Kramer for his contribution in the model compound reaction probes.

REFERENCES

1. Hogan, J. P., *J. Polym. Sci.* **8,** 2637 (1970).
2. Thomas, R., Kerkhof, F. P. J. M., Moulijn, J. A., Medma, J., and deBeer, V. H. J., *J. Catal.* **61,** 559 (1980).
3. Tittarelli, P., Iannibello, A., and Villa, P. L., *J. Solid State Chem.* **37,** 95 (1981).
4. Thomas, R., deBeer, V. H. J., and Moulijn, J. A., *Bull. Soc. Chim. Belg.* **90,** 1349 (1981).
5. Soled, S., Murrell, L. L., Wachs, I. E., and McVicker, G. B., *J. Amer. Chem. Soc. Div. Pet. Chem. Prepr.* **28,** 1310 (1983).
6. Soled, S., Murrell, L. L., Wachs, I. E., McVicker, G. B., Sherman, L. G., Chan, S., Dispenziere, N. C., and Baker, R. T. K., *ACS Symp. Ser.* **279,** 165 (1985).
7. Ogata, E., Kayima, Y., and Ohta, N., *J. Catal.* **29,** 296 (1979).
8. Hattori, H., Asada, N., and Tanabe, K., *Bull. Chem. Soc. Japan* **51,** 1704 (1978).
9. Davis, B. H., *J. Catal.* **55,** 158 (1978).
10. Shibata, K., Kiyoura, T., Kitagawa, J., Sumiyoshi, T., and Tanabe, K., *Bull. Chem. Soc. Japan* **46,** 2985 (1973).
11. Suarez, W., Dumesic, J. A., and Hill, C. G., *J. Catal.* **94,** 408 (1985).
12. Segawa, K., and Hall, W. K., *J. Catal.* **76,** 133 (1982).
13. Yamaguchi, T., Tanaka, Y., and Tanabe, K., *J. Catal.* **65,** 442 (1980).
14. Melchior, M. T., Vaughan, D. E. W., and Jacobson, A. J., *J. Amer. Chem. Soc.* **104,** 4859 (1982).
15. Soled, S., McVicker, G. B., and DeRites, B., "Proceedings 115th NATAS Conf.," p. 417. 1981.
16. McVicker, G. B., Kramer, G. M., and Ziemiak, J. J., *J. Catal.* **83,** 286 (1983).
17. Kramer, G. M., and McVicker, G. B., *Acc. Chem. Res.* **19,** 78 (1986).
18. Ciapetta, F. G., and Henderson, D. J., *Oil Gas J.* **65,** 88 (1967).
19. Brown, H. C., and Johanneson, R. B., *J. Amer. Chem. Soc.* **75,** 16 (1953).
20. Benesi, H. A., and Winquist, B. H. C., "Advances in Catalysis" (D. D. Eley, P. W. Selwood, and P. B. Weisz, Eds.), Vol. 27, p. 96. Academic Press, New York, 1978.
21. Knozinger, H., and Ratnasamy, P., *Catal. Rev. Sci. Eng.* **17,** 31 (1978).
22. Peri, J. B., *J. Phys. Chem.* **69,** 220 (1965).
23. Gorte, R. J., *J. Catal.* **75,** 164 (1982).
24. Mieville, R. L., and Meyers, B. L., *J. Catal.* **74,** 196 (1982).
25. Parry, E. P., *J. Catal.* **2,** 371 (1963).
26. Basilo, M. R., Kantner, T. R., and Rhee, K. H., *J. Phys. Chem.* **68,** 3197 (1964).
27. Basila, M. R., and Kantner, T. R., *J. Phys. Chem.* **70,** 1681 (1966).
28. Peri, J. B., *J. Phys. Chem.* **69,** 211 (1965).
29. Hair, M. L., "Infrared Spectroscopy in Surface Chemistry," Chap. 5. Dekker, New York, 1967.
30. Soled, S., *J. Catal.* **81,** 252 (1983).
31. Soled, S., Murrell, L. L., Wachs, I. E., and McVicker, G. B., "Proceedings of the Petroleum Division," p. 1310. ACS Meeting, Washington, DC, 1983.
32. Bernhole, J., Horsley, J. A., Murrell, L. L., Sherman, L. G., and Soled, S., *J. Phys. Chem.* **91,** 1526 (1987).